Tectonophysics 509 (2011) 191–197

Contents lists available at ScienceDirect

Tectonophysics

journal homepage: www.elsevier.com/locate/tecto

An improved version of the Load/Unload Response Ratio method for forecasting strong aftershocks

Lang-ping Zhang [a,*], Jiancang Zhuang [b]

[a] Institute of Earthquake Science, China Earthquake Administration, Beijing 100036, China
[b] Institute of Statistical Mathematics, 10-3 Midori-cho, Tachikawa, Tokyo 190-8562, Japan

ARTICLE INFO

Article history:
Received 10 August 2010
Received in revised form 19 May 2011
Accepted 9 June 2011
Available online 5 July 2011

Keywords:
Load/Unload Response Ratio (LURR)
Epidemic-type aftershock sequence (ETAS) model
Aftershock forecast
Wenchuan earthquake

ABSTRACT

Temporal clustering and spatial concentration of aftershock sequences can be observed after the occurrence of most major earthquakes. Earthquake clustering effects, such as the rapid decay of aftershocks and second-stage aftershocks, cause large fluctuations in the Load/Unload Response Ratio (LURR). In order to eliminate the influence of such clustering, we introduce a new formula for calculating the LURR, taking the epidemic-type aftershock sequence (ETAS) model as the baseline seismicity model. We have applied the new formula retrospectively to the Wenchuan earthquake sequence in 2008 in China. The results show that the LURR increases slowly to a peak and then decreases sharply before strong aftershocks and that the new LURR performs better than the original LURR.

1. Introduction

It is rather difficult to identify precursors to many geological disasters, such as earthquakes, landslides, and rock bursts, which in fact represent the damage–failure processes of brittle heterogeneous media. From the viewpoint of mechanics, an earthquake is essentially the failure or instability of the focal media accompanied by a rapid release of energy. Yin (1987) proposed a parameter to quantify the preparation process of a large earthquake, namely the Load/Unload Response Ratio (LURR) (Yin and Yin, 1991). The LURR is usually defined as the ratio of the total earthquake energy released during periods when the Coulomb failure stress on the earthquake fault increases and decreases due to tidal effects. Retrospective studies have been carried out for hundreds of cases using the LURR as an earthquake prediction index (Song et al., 2000; Yin et al., 1994; 1995; 1996; 2000). In addition, the LURR method has been investigated in laboratory studies, numerical simulations and from the viewpoint of fundamental physics (see Yin et al., 2002; 2004; 2006; 2008; for recent developments of the LURR method). However, the LURR method has seldom been applied to strong aftershocks, except for an attempt by Wang et al. (1998) to use it to forecast strong shocks in the Jiashi earthquake swarm.

Following a strong earthquake, it is critical to determine as soon as possible whether there will be another of similar or larger magnitude occurring within the next few days. Usually, the Omori–Utsu law or the epidemic-type aftershock sequence (ETAS) model (see Section 3 of this article) is used to describe the temporal clustering and spatial concentration of aftershock sequences and for forecasting the occurrence rate of aftershocks. However, both of these models assume only that the magnitudes of the aftershocks are identically and independently distributed random variables according to the Gutenberg–Richter law, without providing any further information about the magnitudes of coming earthquakes. The LURR can also be used to predict the occurrence of strong aftershocks. However, clustering effects and the rapid decay of aftershocks can lead to large variations in the number of aftershocks occurring in the loading and unloading periods, giving rise to strong variations in the LURR values. In order to eliminate such clustering effects, we use the ETAS model as the baseline model for evaluation of the LURR.

In this paper, we first briefly explain the concepts of the LURR and the ETAS model. We then deduce a new formula for the LURR, based on the ETAS model. This new formula is then applied to forecast strong shocks in the Wenchuan aftershock sequence in 2008 in China.

2. The Load/Unload Response Ratio

From the viewpoint of mechanics, the essence of an earthquake is a failure or instability of the focal media accompanied by a rapid release of energy. Therefore, the preparation process of an earthquake is exactly the damaging process of the focal media. On a microscopic scale, damage mechanisms in geomaterials (rocks) are incredibly

* Corresponding author at: Institute of Earthquake Sciences, China Earthquake Administration, No. 63, Fuxing Road,Haidian District, 100036 Beijing, China. Tel.: +86 10 88015344; +86 138 1156 9323.
E-mail address: zhanglpLURR@gmail.com (L. Zhang).

0040-1951/$ – see front matter © 2011 Published by Elsevier B.V.
doi:10.1016/j.tecto.2011.06.008

complex, and including the initiation, growth, interaction, coalition and cascade of cracks. Such processes are irreversible, nonlinear and far from equilibrium. Even after intensive studies over a period of decades, many fundamental problems in this area still remain unsolved. The inherent difficulty of earthquake prediction stems mainly from the complexity of the damage processes. On a macroscopic scale, stress–strain curves are usually used to comprehensively describe the mechanical behavior of solid materials. A typical stress–strain curve for the focal media (rock) is shown in Fig. 1. When the material is loaded monotonically, it evolves from an elastic phase to a damage formation phase and finally into a failure or destabilization phase. One of the most essential characteristics of the elastic phase is its reversibility, i.e., the strain–stress relation for the loading and unloading processes is reversible. In other words, the loading and unloading moduli are identical in the elastic phase. In contrast, in the damage formation phase, these moduli are different, and the loading and unloading processes are irreversible, indicating a deterioration of the material due to damage.

In order to quantitatively evaluate the difference between the responses of the material to increments and decrements in the load, the response rate X is defined as

$$X = \lim_{\Delta P \to 0} \frac{\Delta R}{\Delta P}, \tag{1}$$

where ΔP and ΔR denote an increment or decrement in the load P and the response R, respectively. The LURR Y is then given by

$$Y = \frac{X_+}{X_-} \tag{2}$$

where X_+ and X_- refer to the response rates when the material is being loaded and unloaded, respectively.

If strain is taken as the response of rock materials to loading or unloading stress, then, as shown in Fig. 1, in the elastic regime, $Y=1$ since $X_+ = X_-$. In the damage formation phase, $X_+ > X_-$, and thus $Y>1$. The more damaged the material is, the larger the Y-value. When the material approaches failure, the Y-value becomes larger and larger and finally tends to infinity. Therefore, the LURR (Y) can be taken as a measure of how close the damaged seismogenic zone is to the failure regime (Yin, 1987; Yin et al., 1994, 1995, 2000). In studies on earthquake prediction, the LURR is calculated directly using the ratio of the total seismic energy released in the loading and unloading periods, i.e., given N earthquakes occurring in a certain time window,

$$Y = \frac{\sum_{i=1}^{N} E_i^{\gamma} I_i}{\sum_{i=1}^{N} E_i^{\gamma} (1 - I_i)}, \tag{3}$$

where E_i denotes the seismic energy released by the ith earthquake. I_i takes values of 1 or 0 if the ith earthquake occurs in the loading or unloading period, respectively, and γ takes values of 0, 1/3, 1/2, 2/3, or 1. When $\gamma=1$, E_i^{γ} simply corresponds to the energy released. When $\gamma=1/2$, E_i^{γ} denotes the Benioff strain. When $\gamma=1/3$ or $\gamma=2/3$, E_i^{γ} represents the linear or areal scale of the seismogenic zone,

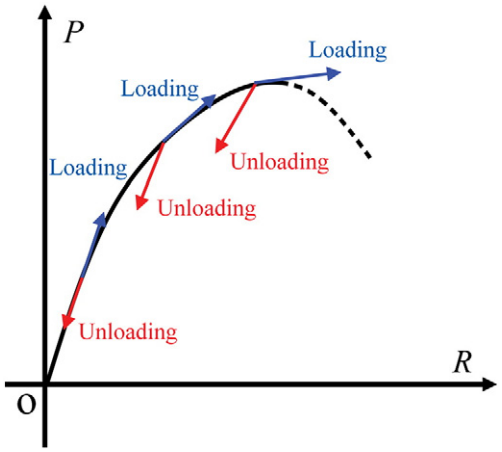

Fig. 1. The stress–strain relation of rock materials.

respectively. Finally, when $\gamma=0$, Y is equal to N_+/N_-, where N_+ and N_- denote the number of earthquakes occurring during the loading and unloading periods, respectively. In the present study, γ is set 1/2, i.e., Y is determined by the Benioff strains released by earthquakes.

The Earth's tides can act as the source of loading and unloading for the earthquake fault, and changes in the loaded stress can be determined by perturbations in the Coulomb failure stress induced by the tides (Yin et al., 1995). The Coulomb failure stress (*CFS*) (e.g., Harries, 1998; Jaeger and Cook, 1976; Resernberg and Simpson, 1992) can be calculated using (without consideration of pore pressure)

$$CFS = \tau_n + f\sigma_n, \tag{4}$$

where σ_n is the normal stress, τ_n denotes the shear stress, f represents the coefficient of internal friction (taken as 0.4 in this paper), and n indicates the direction normal to the fault plane, on which *CFS* reaches its maximum. When the increment in Coulomb failure stress (ΔCFS) is positive, the focal material is regarded as being loaded; otherwise, it is unloaded. As is well known, the crustal stress σ_{ij} consists of the tectonic stress σ_{ij}^T and the tidal stress σ_{ij}^t. Since the magnitude of σ_{ij}^T (10^6–10^8 Pa) far exceeds that of σ_{ij}^t (10^3–10^4 Pa), the directions of the principle stress in the crust and n can be determined from the tectonic stress. However, the daily changes in the tidal stress are much larger than those in the tectonic stress (Vidall et al., 1998). Thus, the daily ΔCFS for the dominant fracture mechanism is mainly due to the tidal stress, which can be calculated with reasonable precision.

Through retrospective inspections on hundreds of earthquake cases, Yin et al. (1994, 1995, 2000) reported that in more than 80% of these cases, the Y-value fluctuates around 1 during the early stage of the seismogenic process, and it starts to increase when the region approaches the onset of a strong earthquake. After reaching a peak value (significantly larger than 1), it usually decreases sharply in a short time before a large earthquake (see earthquake cases in Fig. 2).

3. The epidemic-type aftershock sequence (ETAS) model

Typical aftershock decay is represented by the Omori–Utsu formula which declares that the number of aftershocks per unit time at a time t after the main shock is proportional to $(t+c)^{-p}$, where c and p are constants. This formula was proposed by Utsu (1961) as an extension to the Omori law, based on fitting of a large number of datasets, and remains the most widely used model for typical aftershock rate decay.

However, aftershock activity is not always well predicted by a single Omori–Utsu function, especially when conspicuous secondary activity associated with large aftershocks is included. Ogata (1988) proposed the ETAS model to describe the cascading features of aftershocks. This model has been developed into spatiotemporal versions (e.g., Console et al., 2003; Ogata, 1988; Ogata and Zhuang, 2006) and used as a standard model for testing earthquake-related hypotheses (Helmstetter and Sornette, 2003a,b; Zhuang, 2006; Zhuang et al., 2004, 2008) and forecasting

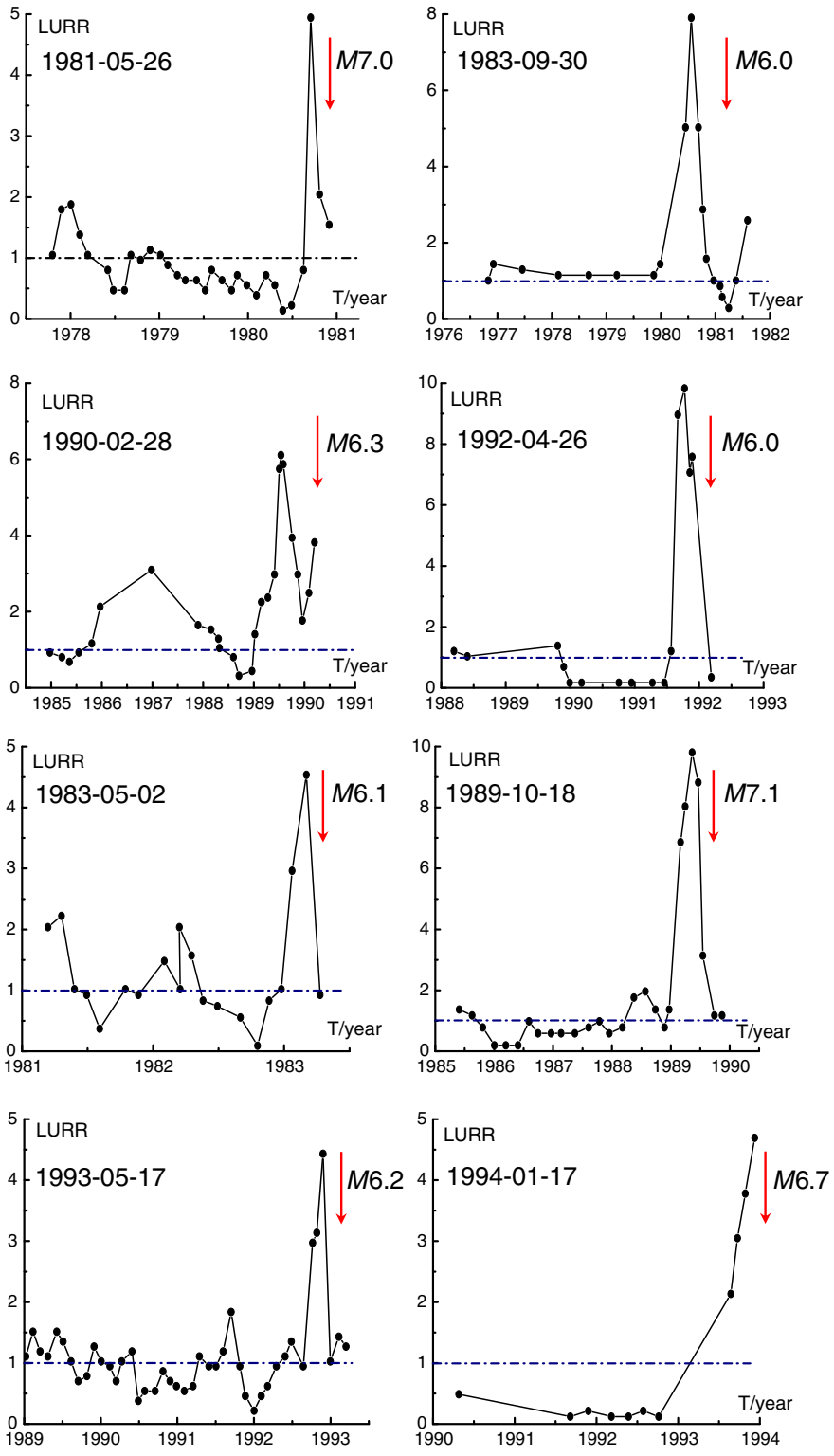

Fig. 2. LURR curves for eight M≥6.0 earthquakes in California, U.S.A., from 1980 to 1994 (c.f., Yin et al., 2000). The tuning parameters for the calculation are given in Yin et al. (2000).

earthquakes using a probability approach (Helmstetter et al., 2006; Vere-Jones, 1998). In this model, every event, irrespective of whether it represents background seismicity or is triggered by a previous earthquake, can trigger its own aftershocks. The occurrence rate is given by a (weighted) superposition of inverse power functions shifted in time, i.e., the time-varying seismicity rate is given by

$$\begin{aligned}\lambda_0(t) &= \lim_{\Delta t\to 0^+}\frac{\Pr\{\text{at least 1 event occurs in } [t,t+\Delta t] | \text{ obeservations before } t\}}{\Delta t},\\ &= \mu + K\sum_{i:t_i<t}\frac{e^{\alpha(m_i-m_0)}}{(t-t_i+c)^p}\end{aligned} \tag{5}$$

where μ (shocks/day) represents the rate of background seismicity, the summation is taken over aftershocks occurring before time t (days), and m_0 represents the cut-off magnitude of the fitted data. The coefficient α (magnitude^{-1}) is a measure of the efficiency of a shock in generating aftershock activity relative to its magnitude. Note that K (shocks/day) is multiplied by $\exp[\alpha(m_i - m_0)]$ for each earthquake i.

Even though it has been shown that earthquake magnitudes exhibit some long-term correlation (Ogata and Abe, 1991), here we simply assume that they are independently identically distributed random variables according to the Gutenberg–Richter law (exponential distribution), i.e., the seismicity rate for an event of magnitude m at a time t, conditional on what happened before t, is

$$\begin{aligned}\lambda_0(t,m) &= \lim_{\Delta t\to 0^+}\lim_{\Delta m\to 0}\frac{\Pr\{\text{at least 1 event occurs in } [(t,t+\Delta t)\times(m,m+\Delta m)]|\ \text{obeservations before } t\}}{\Delta t\Delta m},\\ &= \lambda_0(t)s(m)\end{aligned} \tag{6}$$

where $s(m)=\beta e^{-\beta(m-m_0)}$, $m\geq m_0$, is the probability density form of the Gutenberg–Richter law, and β is linked with the so-called b-value by $\beta = b\log 10$.

Given a set of observation data $\{(t_i, m_i): i=1,\ldots,N\}$ in a period $[0,T]$, the likelihood function with respect to a parameter vector $\Theta=(\mu,K,\alpha,c,p)$ has the standard form (e.g., Daley and Vere-Jones, 2003, Chap. 7)

$$logL(\Theta) = \sum_{i=1}^{N} log\lambda_0(t_i,m_i) - \int_{m_0}^{\infty}\int_0^T \lambda_0(t,m)dtdm\ . \tag{7}$$

We can estimate the model parameters by maximizing the likelihood function, namely, maximum likelihood estimates (MLE) of the model parameter.

4. Combination of the LURR method and the ETAS model

To introduce the loading and unloading responses to changes in the tidally induced forces into earthquake clustering, we use the following model to describe standard seismicity, defined by a conditional intensity

$$\lambda(t,m) = X(t)\lambda_0(t,m) = X(t)\lambda_0(t)s(m) \tag{8}$$

where $\lambda_0(t, m)$ takes the same form as in Eq. (6), and $X(t)$ is the response rate at time t, taking values X_+ and X_- during the loading and unloading periods, respectively.

Given a marked point process equipped with a conditional intensity $\lambda(t, m)$, the following theorem holds (e.g., Zhuang 2006): if $h(t, m)$ is a predictable process, i.e., either a deterministic function or a stochastic function with values determined by observations up to but not including a time t, then

$$E\left[\sum_{i:t_i\in S} h(t_i,m_i)\right] = E\left[\int_M\int_S h(t,m)\lambda(t,m)dmdt\right] \tag{9}$$

holds for any period S, where M represents the magnitude range.

Taking $h(t, m)=f(m)/\lambda_0(t_i)$, where $f(m)$ is a pre-defined function of m, and denoting by $|S_+|$ the length of the loading period, S_+, we have

$$\begin{aligned}\mathrm{E}\left[\sum_{i:t_i\in S_+} f(m_i)/\lambda_0(t_i)\right] &= \mathrm{E}\left[\int_M\int_{S_+}\frac{f(m)\lambda(t,m)}{\lambda_0(t)}dmdt\right]\\ &= \mathrm{E}\left[\int_M\int_{S_+} f(m)s(m)X(t)dmdt\right]\ .\\ &= X_+|S_+|\left[\int_M f(m)s(m)dm\right]\\ &= X_+|S_+|\mathrm{E}[f(m)]\end{aligned} \tag{10}$$

Similarly,

$$\mathrm{E}\left[\sum_{i:t_i\in S_-} f(m_i)/\lambda_0(t_i)\right] = X_-S_-\mathrm{E}[f(m)], \tag{11}$$

where S_- is the length of the unloading period. Thus, combining Eqs. (2), (10) and (11), Y can be obtained as

$$Y = \frac{X_+}{X_-} = \frac{|S_-|\mathrm{E}\left[\sum_{i:t_i\in S_+} f(m)/\lambda_0(t_i)\right]}{|S_+|\mathrm{E}\left[\sum_{i:t_i\in S_-} f(m)/\lambda_0(t_i)\right]} \approx \frac{|S_-|\sum_{i:t_i\in S_+} f(m_i)/\lambda_0(t_i)}{|S_+|\sum_{i:t_i\in S_-} f(m_i)/\lambda_0(t_i)}\ . \tag{12}$$

If we let $f(m)=1$, (12) gives the ETAS version of Y_0. Applications and mathematical properties of such reciprocal-lambda residuals related to point-process data can be also found in Schoenberg (2004),

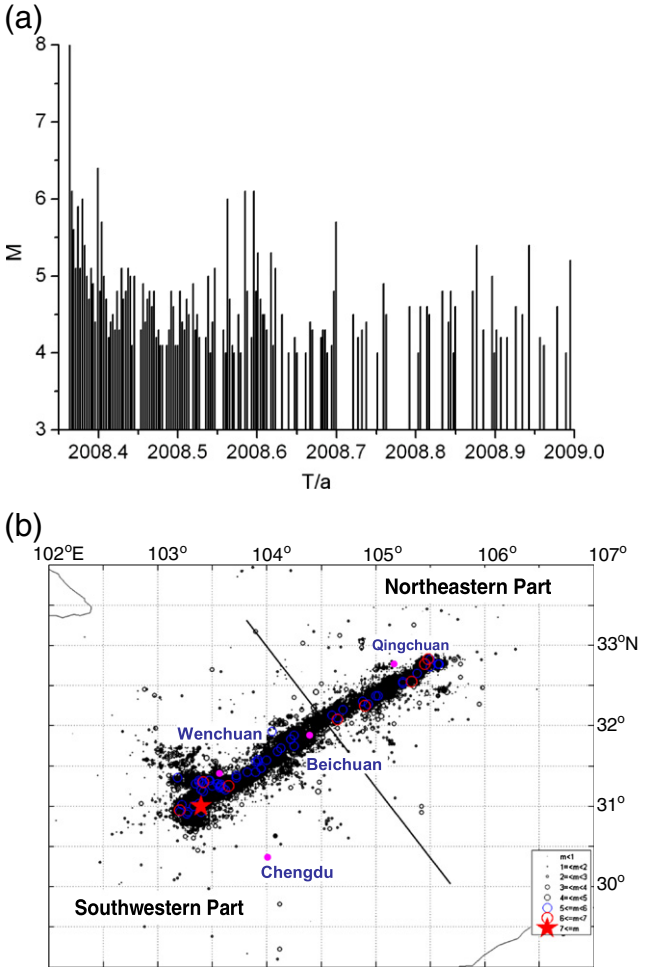

Fig. 3. (a) Magnitude against occurrence time for the Wenchuan earthquake and its aftershocks; (b) distribution of epicenter locations for the Wenchuan earthquake and its aftershocks.

Veen and Schoenberg (2005), Zhuang et al. (2005) and Zhuang (2006). In this study, we let $f(m)$ be the Benioff strain, and (12) gives the corresponding ETAS version of Y_2, i.e., our new LURR formula becomes

$$Y_2 \approx \frac{|S_-| \sum_{i:t_i \in S_+} E_i^{1/2} / \lambda_0(t_i)}{|S_+| \sum_{i:t_i \in S_-} E_i^{1/2} / \lambda_0(t_i)} . \quad (13)$$

The likelihood function for this model has the same form as the ETAS model given by Eq. (7) except that λ_0 is replaced by $\lambda(t, m)$. Since $X(t)$ is unknown, we cannot use the MLE method to obtain parameters in this model. However, we can still fit the normal ETAS model to observed earthquake data to estimate λ_0 and then substitute $\lambda_0(t, m)$ into Eq. (13) to get Y_2.

5. Data analysis

The Wenchuan earthquake (MS8.0, 31.0°N, 103.4°E) occurred at 14:28, May/12/2008 in Sichuan Province, China. It was followed by seven aftershocks with magnitudes $M \geq 6.0$ and 60 with magnitudes $M \geq 5.0$ during the period from 05/12/2008 to 12/31/2008. Fig. 3 shows a magnitude–time plot and a map of the epicenter locations of the aftershocks.

The rupture of this great earthquake started at Wenchuan, and then extended north–northeast along the Longmenshan thrust belt. The faulting geometry along the rupture appeared to be complex. Reverse and right-slip components were of comparable magnitude along the SW portion of the rupture, but right-slip dominated the NE portion (Burchfiel et al., 2008; Zhang et al., 2008). The centroid moment tensor (CMT) solutions for the fault system are different between the SW and NE portions along the fault direction. According to a report by the Seismic Networks Center, China Earthquake Administration, the CMT solutions are (strike: 229°, dip: 33°, slip: 141°, depth: 10 km) for the SW part of the fault and (strike: 229°, dip: 33°, slip: 180°, depth: 10 km) for the NE part.

We first fit the ETAS model to all data of $M \geq 2.1$ from the whole aftershock region and the whole time period from 05/12/2008 to 12/31/2008. The estimated parameters are $\hat{\mu} = 14.729$ (events/day), $\hat{K} = 0.109$ (events/day), $\hat{c} = 0.106$ day, $\hat{\alpha} = 0.343$, and $\hat{p} = 1.621$. Because this earthquake has two different focal mechanisms, we divide the whole aftershock region into two parts, the northeastern part and the southwestern part, separated by a straight line through points (33°N, 104°E) and (29.5°N, 106°E) (Fig. 3(b)). Both the original and new LURR values for each part of the aftershock region are calculated from 05/12/2008 to 12/31/2008 using a 4-day moving time window and a 1-day moving step. The resulting variations in the original and new LURR values for the southwestern region are shown in Fig. 4.

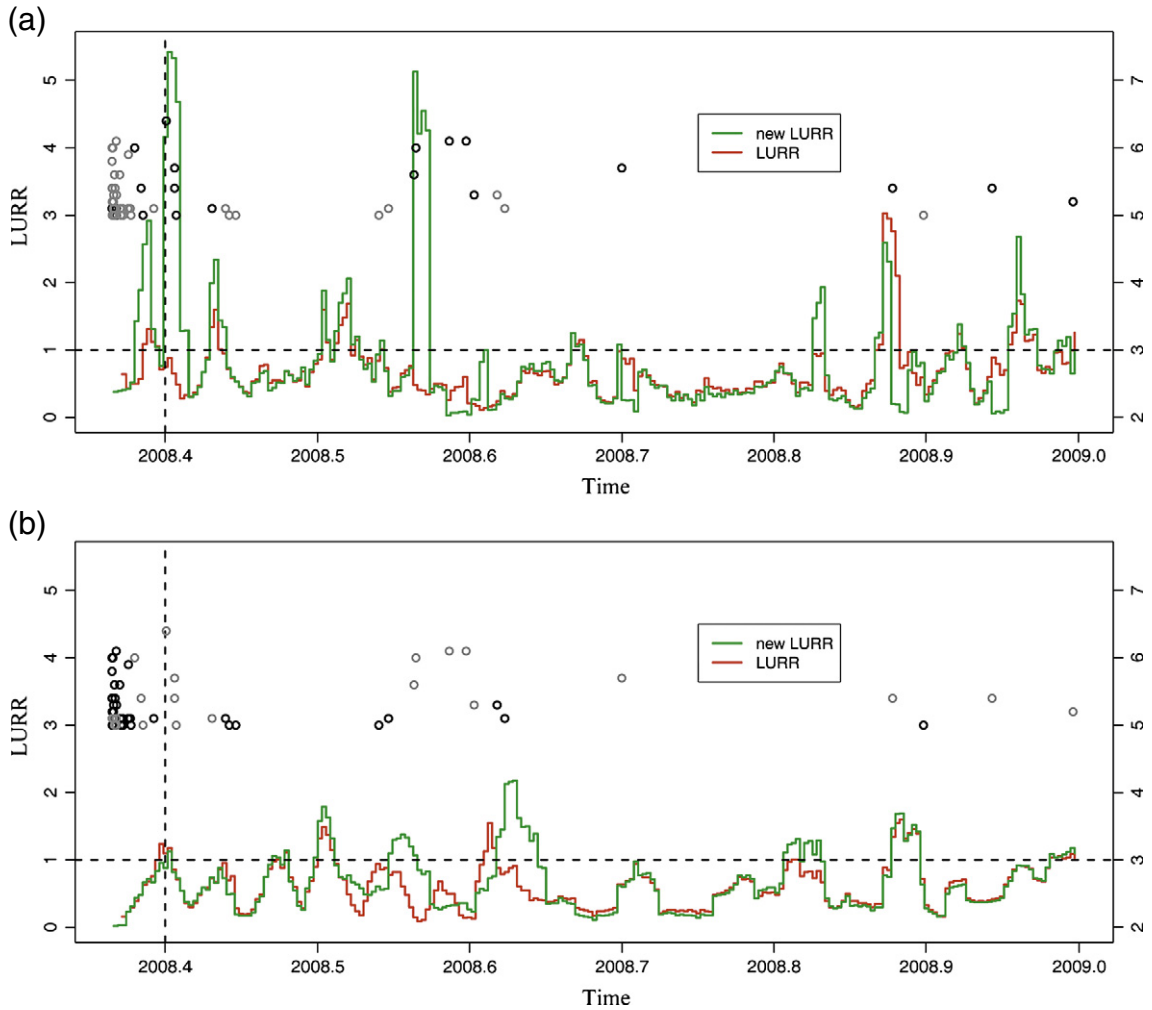

Fig. 4. Time evolution of original and new LURR values for (a) NE part and (b) SW part of Wenchuan earthquake and aftershock region. Earthquakes with magnitude $M \geq 5.0$ are superimposed, with black circles representing large aftershocks in the same part of the aftershock region and gray circles in the other part.

We start our prediction experiment after 5/26/2008 (2008.398 in year) because many events of $M \geq 2.1$ are missing in the early period of the mainshock. From Fig. 4a, we can see that, in the NE part, the biggest difference between the curves for the new and original LURR values is that there are two peaks in the new LURR curve in the first half of the prediction time period, each followed by a cluster of large aftershocks, whereas the original LURR curve does not show any significant variation. In the second half of the prediction period, there are two smaller peaks in both the new and the original LURR curves, each followed by an isolated strong aftershock. Among the large aftershocks, there are no LURR peaks corresponding to the two events which occurred on 09/21/2008 (M5.7) and 12/10/2008 (M5.4).

In the SW part, the LURR values are much smaller than in the NE part and the seismicity level is also lower. Large aftershocks in this part can be classified into four groups based on their occurrence times: three doublets and one singleton. It can be seen that the singleton on 12/23/2008 (M5.0) is well predicted by both the new and original LURR curves (Fig. 4b). The third group is predicted by the original LURR, but not by the new LURR. The predictions for the first and the second groups are not significant.

To carry out our prediction experiment, we first define an alarm level function as the highest LURR value in the last $\Delta = 14$ days (Figs. 5a and c), and then use the Molchan error diagram (Molchan, 1990, 1991, 1997, 2003; Molchan and Kagan, 1992) to evaluate the performance of the new and original LURRs. The Molchan error diagram is constructed as follows. For every possible threshold of the alarm level function, time periods with alarm levels above the threshold are designed as alarm periods, and a curve is plotted of the fraction of earthquakes failed to predict, ν, against the fraction of time occupied by the alarm, τ. The resulting diagram provides a comprehensive summary of the performance of such alarms. In the case of a completely random guess, as it is easy to see, $\nu = 1 - \tau$, and the diagram is a straight line joining the points (0, 1) and (1, 0). A better alarm strategy than a completely random guess would have a ν–τ curve below this straight line whereas a worse strategy has a curve above it. Zechar and Jordan (2008) defined the Area Skill Score (ASS) as the area enclosed by the ν–τ curve and the straight line $\nu = 1 - \tau$, which is positive when the ν–τ curve is below the straight line and negative when it is above it.

Molchan error diagrams for the NE and SW parts of the aftershock region are shown in Fig. 5b and d, respectively. From Fig. 5b, it can be seen that the original LURR curve is marginally better than random guessing while the new LURR is significantly better. For the SW part, both LURR methods show better performance than random guessing and the original LURR has a higher area skill score.

Similar results were obtained for Δ values in the range 5 to 25 days, with the best performance being obtained for $\Delta = 12 \sim 18$ days. Another interesting result is that if the LURR values from one part are used to predict strong aftershocks in the entire aftershock region, the Molchan error diagram also indicates a significant improvement over random guessing.

In addition to the change in seismicity rate caused by the mainshocks, there are many other factors influencing the calculation of the LURR. For example, the time for nucleation of a fracture event for a given stress and stress rate is unknown and could range anywhere from seconds to days. Also, once an earthquake occurs, it changes the Coulomb stress level on the fault. All of these factors could obscure the daily tidal correlation and further studies are required to improve the prediction performance of the LURR method. Numerically, there are also some parameters that can be "tuned" during retrospective forecasting, including the size and shape of the region considered. In the current application of the LURR, the nucleation time might not be expected to be such a large issue since, after the main rupture, the physical characteristics of the zone of fractured rock

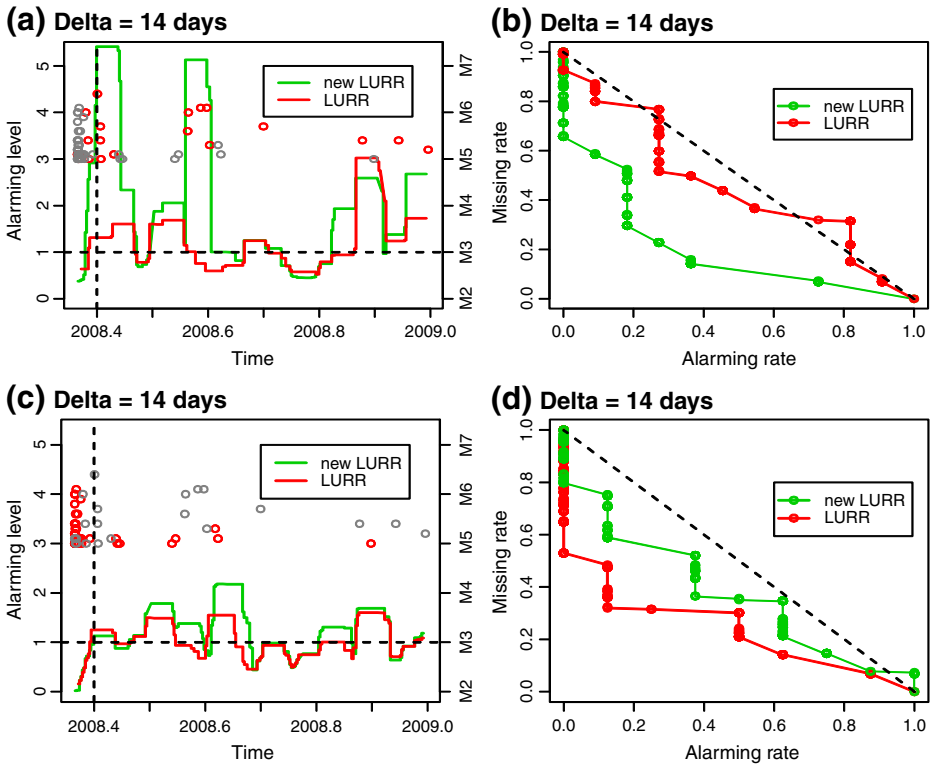

Fig. 5. (a) Alarm levels generated by the new and original LURR values for the NE part of the aftershock region and (b) Molchan error diagram. (c) and (d) are corresponding plots for the SW part of the aftershock region.

would be quite different and it is likely that the rock would respond more quickly to changes in the strain rate. Also, the area chosen for analysis is defined by the aftershocks themselves and is not as arbitrary as in the case of using regional seismicity to forecast a yet to occur major earthquake.

In summary, based on the above analysis of two datasets and three regions, it was found that the new LURR peaks are in better agreement with the occurrences of strong aftershocks than the original ones in the northeastern part of the Wenchuan aftershock region, while the original LURR peaks show slightly better agreement in the southwestern part.

6. Concluding remarks

Temporal clustering in aftershock sequences affects the calculation of the original LURR. However, this effect can be eliminated by using the ETAS model as the baseline model in the calculations. The new formula, combining the LURR and ETAS models, was applied to the great 2008 Wenchuan earthquake. Comparisons between the prediction performance of the original and new computation methods were made using Molchan error diagrams. The results indicated that both LURR values usually exhibited a peak about two weeks before the occurrence of strong aftershocks. The new LURR curves are likely to be in better agreement with actual aftershock occurrence than the original ones, and exhibit much higher peaks. These results suggest that this combined method could be used as a prediction index for strong aftershocks.

Acknowledgments

We gratefully acknowledge the support from the National Natural Science Foundation of China (grant no. 41004018) and the Basic Research Foundation of the Institute of Earthquake Science, China Earthquake Administration (grant no. 02092425). This work was initiated when J. Zhuang was visiting the Institute of Geophysics, China Earthquake Administration, by invitation of Prof. Zhongliang Wu and Dr. Changsheng Jiang. We thank Prof. Yosihiko Ogata from the Institute of Statistical Mathematics for helpful discussions.

References

B.C. Burchfiel, L.H. Royden, R.D. vander Hilst, et al. (2008), A geological and geophysical context for the Wenchuan earthquake of 12 May 2008, Sichuan, People's Republic of China. GSA Today, July, 4-11.

Console, R., Murru, M., Lombardi, A.M., 2003. Refining earthquake clustering models. Journal of Geophysical Research 108 (B10), 2468. doi:10.1029/2002JB002130.

Daley, D., Vere-Jones, D., 2003. An Introduction to Theory of Point Processes, Volume I. Springer, New York.

Harries, R.A., 1998. Introduction to special section: stress triggers, stress shadows, and implication for seismic hazard. Journal of Geophysical Research 103, 24,347–24,358.

Helmstetter, A., Sornette, D., 2003a. Predictability in the Epidemic-Type Aftershock Sequence model of interacting triggered seismicity. Journal of Geophysical Research 108 (B10), 2482. doi:10.1029/2003JB002485.

Helmstetter, A., Sornette, D., 2003b. Foreshocks explained by cascades of triggered seismicity. Journal of Geophysical Research 108 (B10), 2457. doi:10.1029/2003JB002409.

Helmstetter, A., Kagan, Y.Y., Jackson, D.D., 2006. Comparison of short-term and time-independent earthquake forecast models for southern California. Bulletin of the Seismological Society of America 96 (1), 90–106.

Jaeger, J.C., Cook, N.G.W., 1976. Fundamentals of Rock Mechanics. Chapman and Hall, London, pp. 78–79.

Molchan, G.M., 1990. Strategies in strong earthquake prediction. Physics of The Earth and Planetary Interiors 61 (1.2), 84–98.

Molchan, G.M., 1991. Structure of optimal strategies in earthquake prediction. Tectonophysics 193 (4), 267–276.

Molchan, G.M., 1997. Earthquake prediction as a decision-making problem. Pure and Applied Geophysics 149 (1), 233–247.

Molchan, G.M., 2003. In: Keilis-Borok, V.I., Soloviev, A.A. (Eds.), Earthquake Prediction Strategies: A Theoretical Analysis, in NonlinearDynamics of the Lithosphere and Earthquake Prediction. Springer, Heidelberg, pp. 208–237.

Molchan, G.M., Kagan, Y.Y., 1992. Earthquake prediction and its optimization. Journal of Geophysical Research 97 (B4), 4823–4838.

Ogata, Y., 1988. Statistical models for earthquake occurrences and residual analysis for point processes. Journal of the American Statistical Association 83 (401), 9–27.

Ogata, Y., Abe, K., 1991. Some statistical features of the long-term variation of the global and regional seismic activity. International Statistical Review 59 (2), 139–161.

Ogata, Y., Zhuang, J., 2006. Space–time ETAS models and an improved extension. Tectonophysics 413 (1–2), 13–23.

RESERNBERG, P.A., SIMPSON, R.W., 1992. Response of regional seismicity to the static stress change produced by the Loma Prieta Earthquake. Science 255, 1687–1690.

Schoenberg, F.P., 2004. Multidimensional residual analysis of point process models for earthquake occurrences. Journal of the American Statistical Association 98, 789–795. doi:10.1198/016214503000000710.

Song, Z.P., Yin, X.C., Wang, Y.C., Xu, P., Xue, Y., 2000. The tempo-spatial evolution characteristics of the Load/Unload Response Ratio before strong earthquakes in California of America and its predicting implications. Acta Seismologica Sinica 22 (6), 588–595 (in Chinese).

Utsu, T., 1961. A statistical study on the occurrence of aftershocks. Geophysical Magazine 30, 521–605.

Veen, A., Schoenberg, F.P., 2005. Assessing spatial point process models for California earthquakes using weighted K-functions: analysis of California earthquakes. In: Baddeley, A., Gregori, P., Mateu, J., Stoica, R., Stoyan, D. (Eds.), Case Studies in Spatial Point Process Models. Springer, NY, pp. 293–306.

Vere-Jones, D., 1998. Probabilities and information gain for earthquake forecasting. Computational Seismology 30, 248C263.

Vidall, J.E., Agnew, D.C., Johnston, M.J.S., Oppenheimer, D.H., 1998. Absence of earthquake correlation with earth tides: an indication of high preseismic fault stress rate. Journal of Geophysical Research 103, 24,567–24,572.

Wang, H.T., Peng, K.Y., Zhang, Y.X., Wang, Y.C., Yin, X.C., 1998. Characters of variation of LURR during the earthquake sequence of Xinjiang. Chinese Sciences Bulletin 43, 1752–1755.

YIN, X.-c, 1987. Explore new approach to earthquake prediction. Earthquake Research in China 3 (10), 1–7 (in Chinese).

Yin, X.C., Yin, C., 1991. The precursor of instability for nonlinear system and its application to earthquake prediction. Science in China. Series B 5, 512–518 (inChinese).

Yin, X.C., Chen, X.Z., Song, Z.P., 1994. The Load/Unload response Ratio (LURR) theory and its application to earthquake prediction. Journal of Earthquake Prediction Research 3 (3), 325–333.

Yin, X.C., Chen, X.Z., Song, Z.P., Yin, C., 1995. A new approach to earthquake prediction—the Load/Unload Response Ratio (LURR) theory. Pure and Applied Geophysics 145 (3–4), 701–715.

Yin, X.C., Chen, X.Z., Song, Z.P., Wang, Y.C., 1996. The temporal variation of LURR in Kanto and other regions of Japan and its application to earthquake prediction. Earthquake Research in China 12 (3), 331–334 (in Chinese).

Yin, X.C., Wang, Y.C., Peng, K.Y., Bai, Y.L., Wang, H.T., Yin, X.F., 2000. Development of a new approach to earthquake prediction: Load/Unload Response Ratio (LURR) theory. Pure and Applied Geophysics 157 (11–12), 2365–2383.

Yin, X.C., Mora, P., Peng, K.Y., Weatherly, D., 2002. Load–unload response ratio and accelerating moment/energy release critical region scaling and earthquake prediction. Pure and Applied Geophysics 159 (9), 2511–2523.

Yin, X.C., Yu, H.Z., Victor, K., Xu, Z.Y., Wu, Z.S., Li, M., Peng, K.Y., Surgey, E., Li, Q., 2004. Load–Unload Response Ratio (LURR), Accelerating Energy release (AER) and state vector evolution as precursors to failure of rock specimens. Pure and Applied Geophysics 161 (11–12), 2405–2416. doi:10.1007/s00024-004-2572-8.

Yin, X.C., Zhang, L.P., Zhang, H.H., Yin, C., Wang, Y.C., Zhang, Y.X., Peng, K.Y., Wang, H.T., Song, Z.P., Yu, H.Z., Zhuang, J., 2006. LURR's twenty years and its perspective. Pure and Applied Geophysics 163 (11–12), 2317–2341. doi:10.1007/s00024-006-0135-x.

Yin, X.C., Zhang, L.P., Zhang, Y.X., Peng, K.Y., Wang, H.T., Song, Z.P., Yu, H.Z., Zhang, H.H., Yin, C., Wang, Y.C., 2008. The newest development of Load–Unload Response Ratio (LURR). Pure and Applied Geophysics 165 (3–4), 711–722. doi:10.1007/s00024-008-0314-z.

Zechar, J.D., Jordan, T.H., 2008. Testing alarm-based earthquake predictions. Geophysical Journal International 172 (2), 715–724. doi:10.1111/j.1365-246X.2007.03676.x.

Zhang, P.Z., Xu, X.W., Wen, X.Z., et al., 2008. Slip rates and recurrence intervals of the Longmen Shan active fault zone, and tectonic implications for the mechanism of the May 12 Wenchuan earthquake, 2008, Sichuan, China. Chinese Journal of Geophysics 51 (4), 1066–1073 (in Chinese with English abstract).

Zhuang, J., 2006. Second-order residual analysis of spatiotemporal point processes and applications in model evaluation. Journal of the Royal Statistical Society: Series B (Statistical Methodology) 68 (4), 635–653. doi:10.1111/j.1467-9868.2006.00559.x.

Zhuang, J., Ogata, Y., Vere-Jones, D., 2004. Analyzing earthquake clustering features by using stochastic reconstruction. Journal of Geophysical Research 109 (B5), B05301. doi:10.1029/2003JB002879.

Zhuang, J., Ogata, Y., Vere-Jones, D., 2005. Diagnostic Analysis of Space–Time Branching Processes for Earthquakes. In: Baddeley, A., Gregori, P., Mateu, J., Stoica, R., Stoyan, D. (Eds.), Chap. 15 (Pages 275–290) of Case Studies in Spatial Point Process Models. Springer-Verlag, New York. 320 pages.

Zhuang, J., Christophersen, A., Savage, M.K., Vere-Jones, D., Ogata, Y., Jackson, D.D., 2008. Differences between spontaneous and triggered earthquakes: their influences on foreshock probabilities. Journal of Geophysical Research 113, B11302. doi:10.1029/2008JB005579.